

Figure Captions

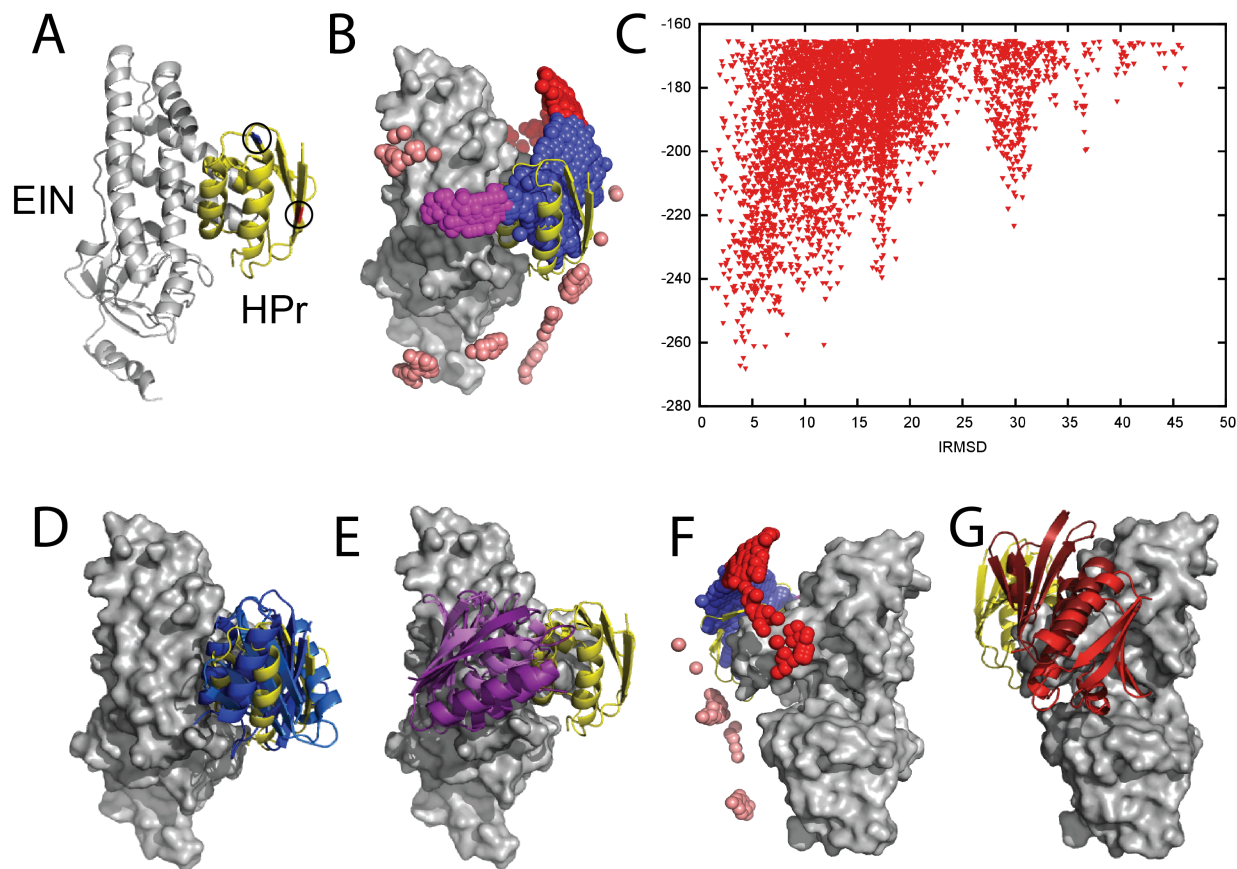


Figure 1 Docking results for the EIN - HPr complex. Unbound structures were used both for the receptor, EIN (chain A from PDB entry 1ZYM) and for the ligand, HPr (chain P from PDB entry 2JEL). Encounter complexes were generated using fast Fourier transform (FFT) based sampling. **(A)** Cartoon of the specific complex formed by EIN and HPr, shown in grey and yellow, respectively. The locations of the paramagnetic tags E5C-EDTA-Mn⁺ and E32C-EDTA-Mn²⁺ on HPr are encircled and are shown in red and blue, respectively. **(B)** Centers of HPr structures in the encounter complex ensemble. Colors indicate classification as follows (8): blue, Class I (i.e., overlapping with the specific complex); magenta, patch 1 of Class II (i.e., non-overlapping) positions; red, patch 2 of Class II positions; and pink, additional Class II position outside the main patches. **(C)** Ligand IRMSD versus PIPER energy score. **(D)** Two representative HPr poses, colored light blue and dark blue, from Class I. **(E)** Two representative HPr poses (in different shades of magenta) from Patch 1 of Class II. **(F)** View of the EIN - HPr complex and the centers of HPr poses after rotating 180° around the vertical axis (the bound HPr is now on the left side, almost completely hidden by EIN). **(G)** Representative HPr poses (in different shades of red) from Patch 2 of Class II, shown in the rotated view.

The following figure supplements are available for Figure 1:

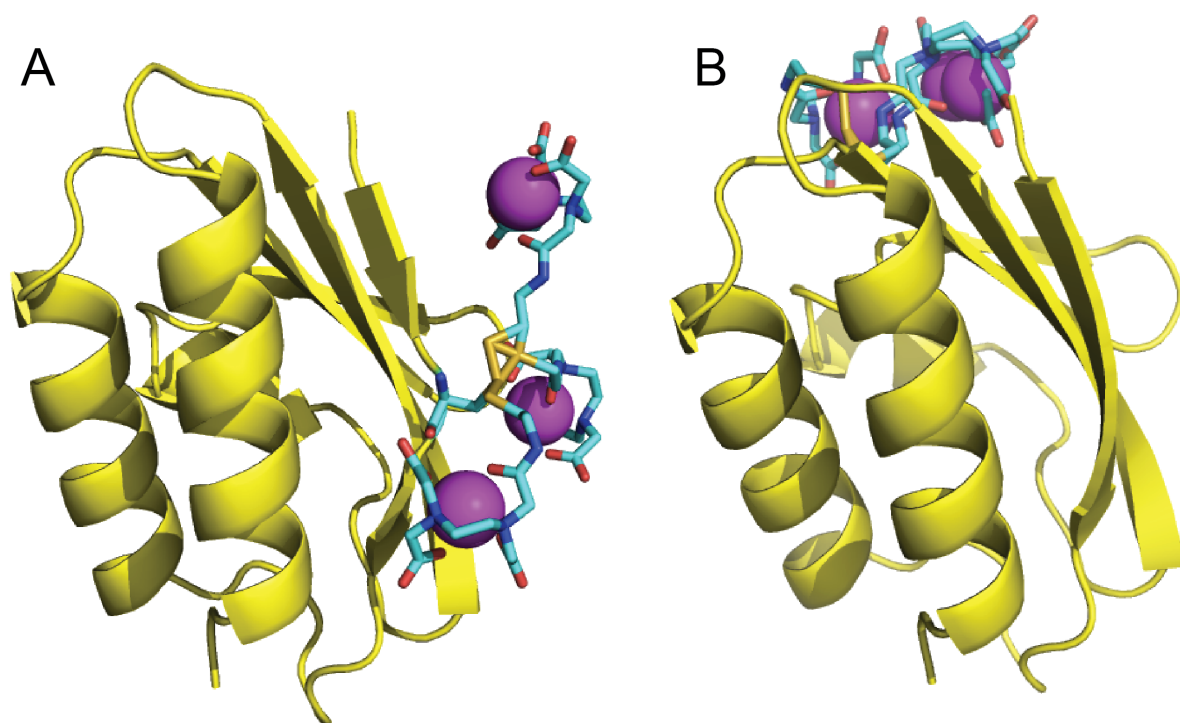


Figure supplement 1. Rotamers of the paramagnetic labels E5C-EDTA-Mn²⁺ and E32C-EDTA-Mn²⁺ on HPr.

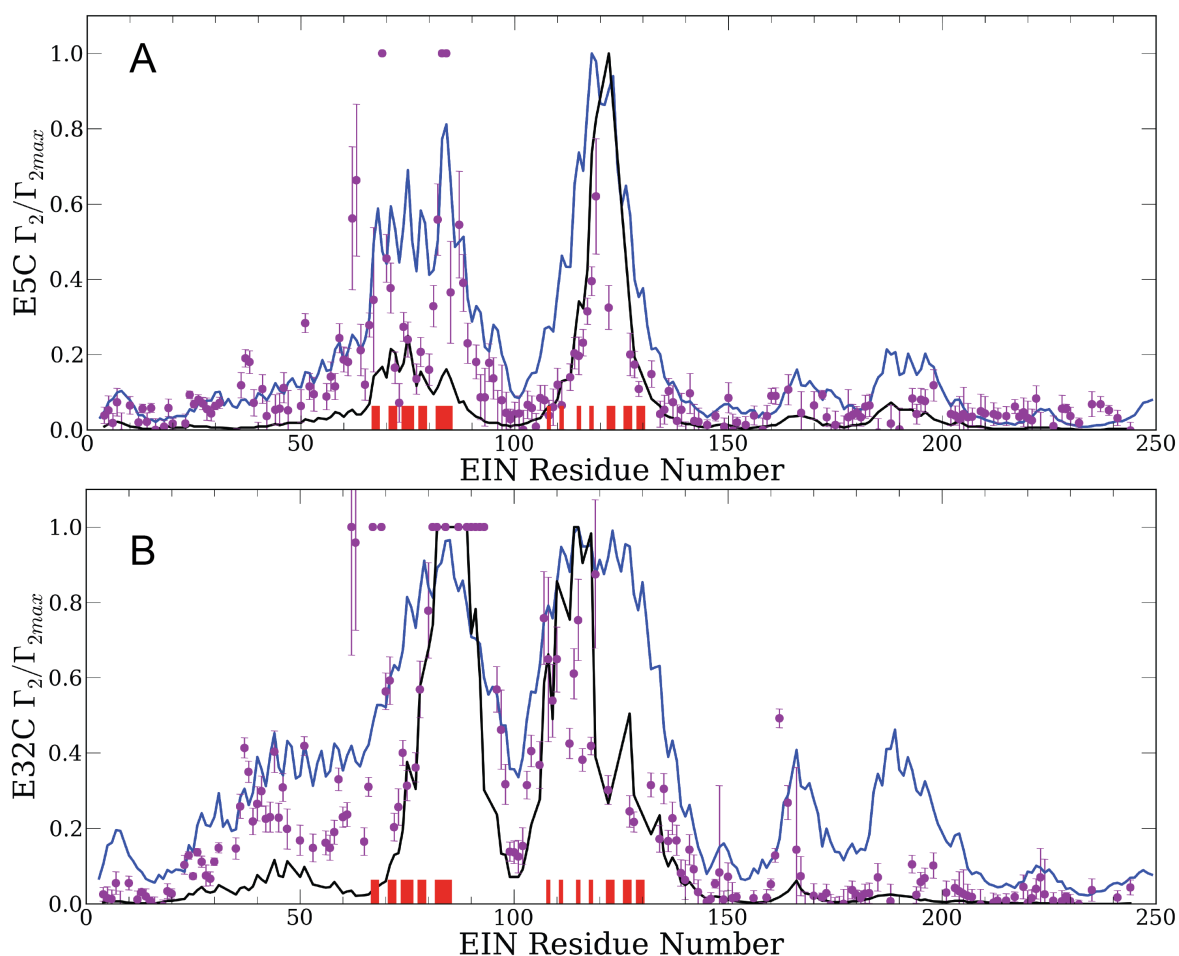


Figure 2 Normalized intermolecular PRE profiles for the EIN - HPr complex. PRE measurements were carried out at 300 mM EIN, 300 mM HPr, and 150 mM NaCl (**Fawzi et al. 2010**). Theoretical intermolecular PREs, calculated only from the coordinates of the specific EIN/HPr complex, are shown as black lines. Calculated PRE values, based on all generated encounter complexes, are shown as blue lines, and reveal substantial contributions by the non-specific structures. The experimental PRE rates (Γ_2) are displayed as filled-in magenta circles. Points representing Γ_2 values that were too large ($>60 \text{ s}^{-1}$) to be determined accurately are placed at the saturation level $\Gamma_2/\Gamma_{2max}=1$. Interface residues are indicated by red ticks on the x-axis. **(A)** Results for EIN/HPr-E5C-EDTA- Mn^{2+} complexes. **(B)** Results for EIN/HPr-E32C-EDTA- Mn^{2+} complexes.

The following figure supplements are available for Figure 2:

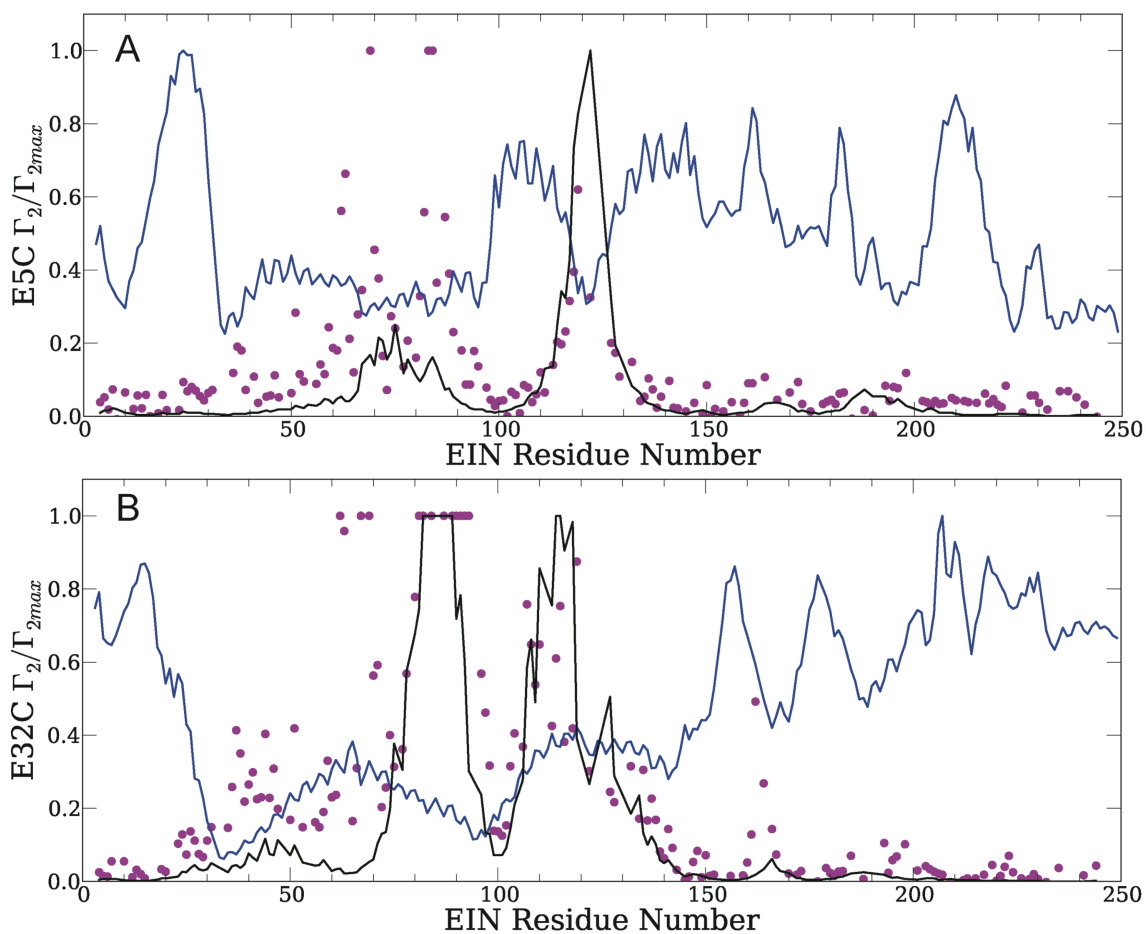


Figure supplement 1. Theoretical PRE profiles for the EIN/HPr complex, based on complexes generated using only the van der Waals energy for scoring.

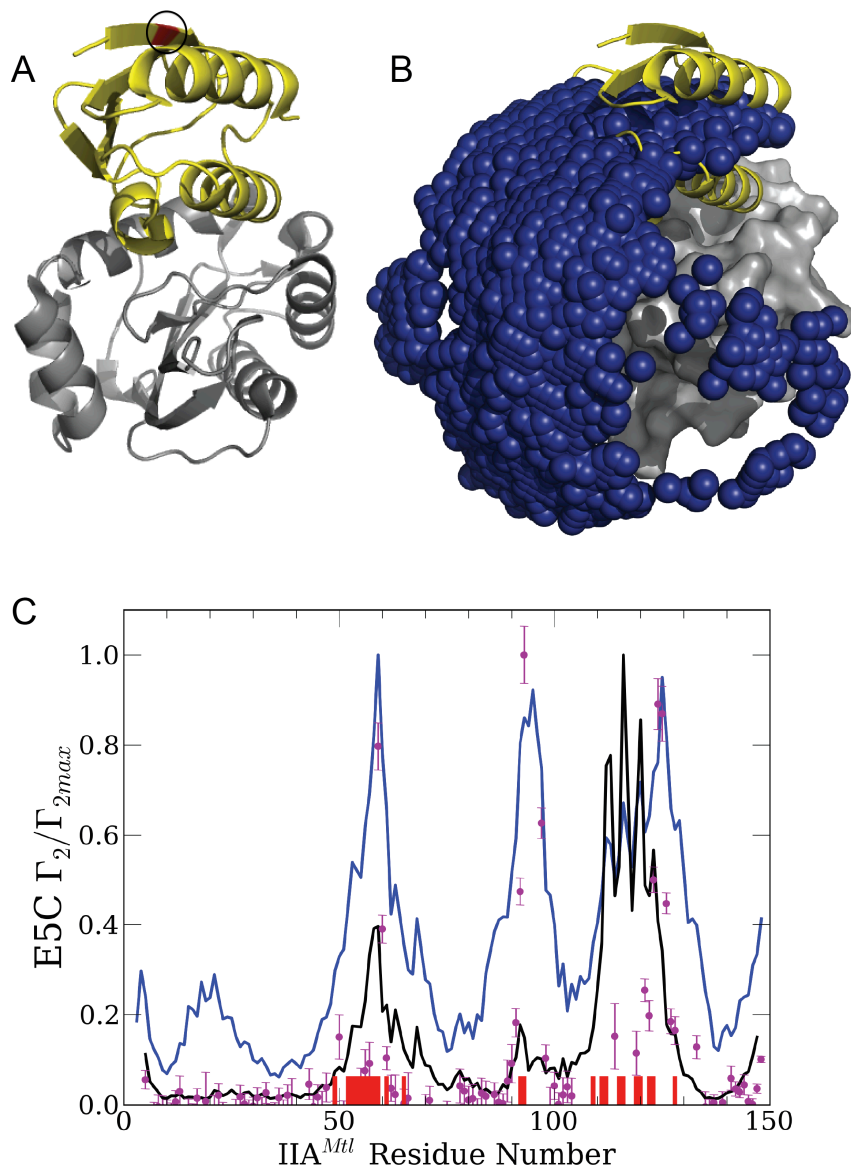


Figure supplement 2. Normalized intermolecular PRE profiles and encounter complexes for the $IA^{Mannitol}$ / HPr interactions. **(A)** Normalized intermolecular PRE profiles for the $IA^{Mannitol}$ / HPr complex. Theoretical intermolecular PREs, calculated only from the coordinates of the specific $IA^{Mannitol}$ / HPr complex, are shown as black lines. Calculated PRE values, based on all generated encounter complexes, are shown as blue lines, and reveal substantial contributions by the non-specific structures. The experimental PRE rates (Γ_2) are displayed as filled-in magenta circles. Points representing Γ_2 values that were too large (>60 s $^{-1}$) to be determined accurately are placed at the saturation level $\Gamma_2/\Gamma_{2max}=1$. Interface residues are indicated by red ticks on the x-axis. **(B)** Centers of HPr structures, shown as blue spheres, in the encounter complex ensemble. These structures were used for back-calculating the theoretical PRE profile (blue curve) shown in Figure A. The receptor, $IA^{Mannitol}$, and the ligand, HPr, in their native binding pose are shown as grey solid and yellow cartoon, respectively.

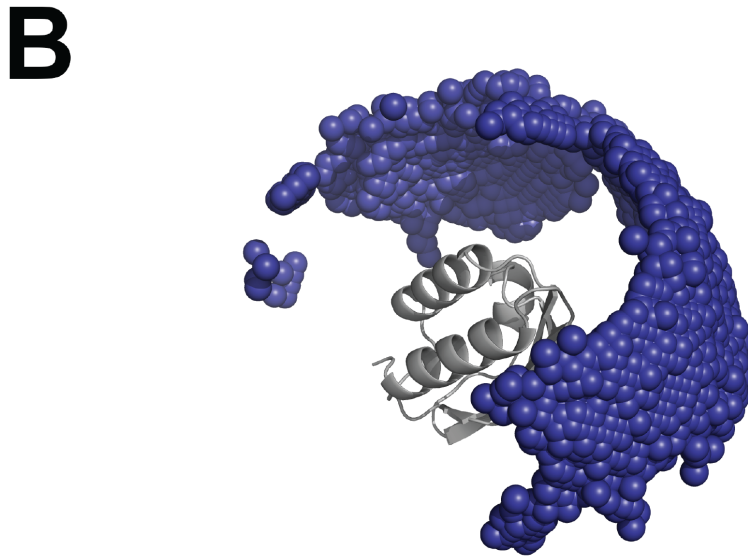
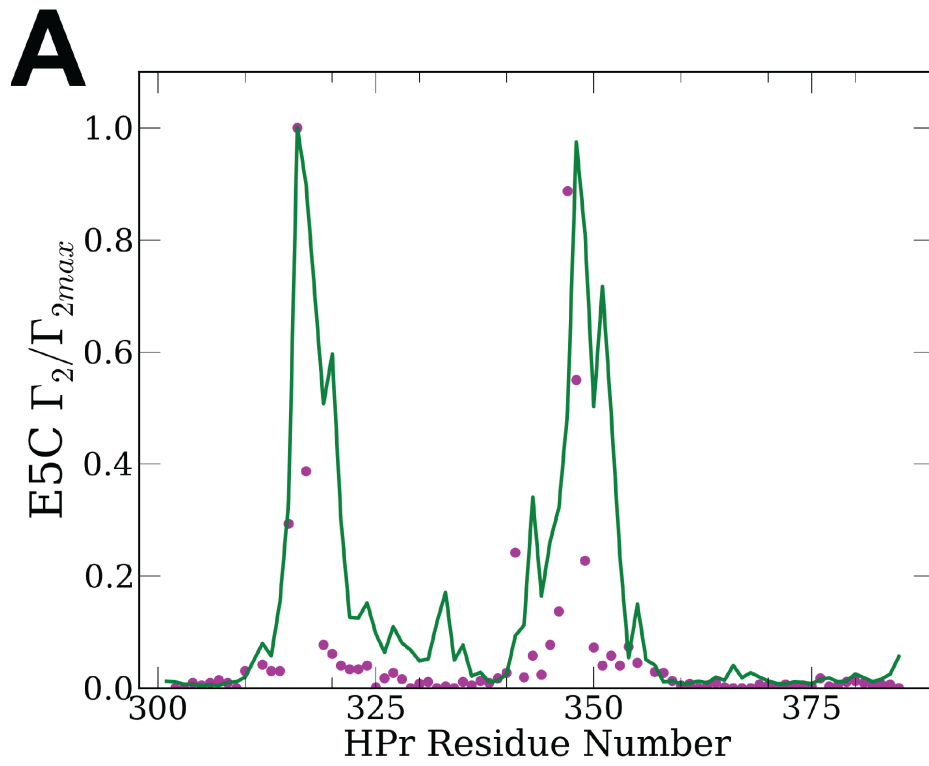


Figure supplement 3. Encounter complexes for the HPr / HPr interaction. (A)

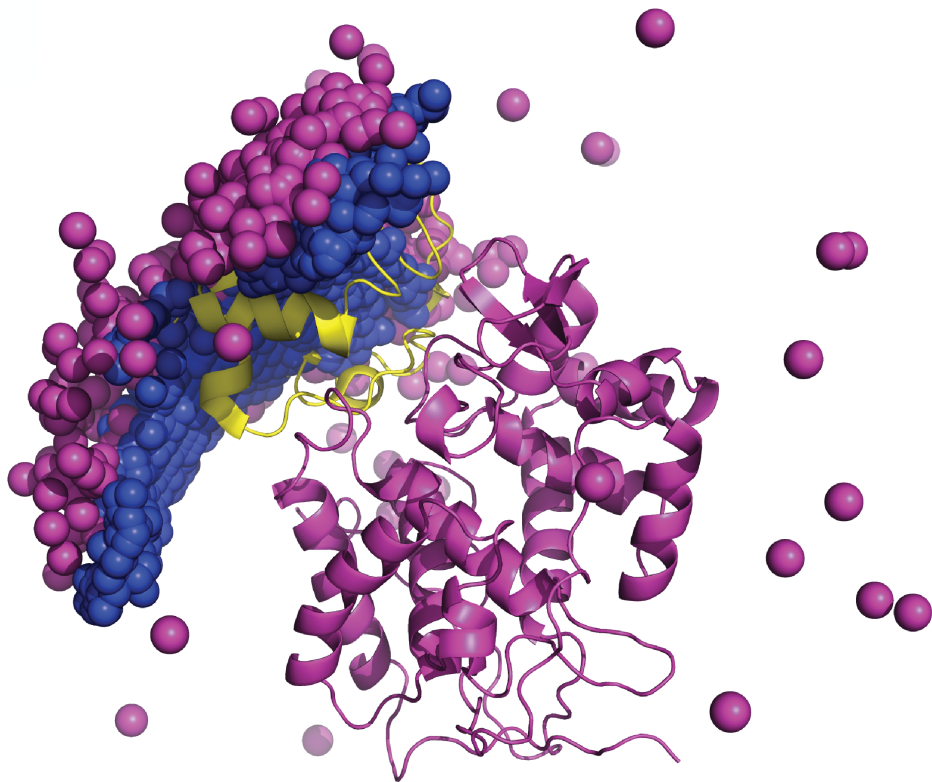


Figure supplement 4 Encounter complexes in the Cytochrome c / Cytochrome c peroxidase interactions.

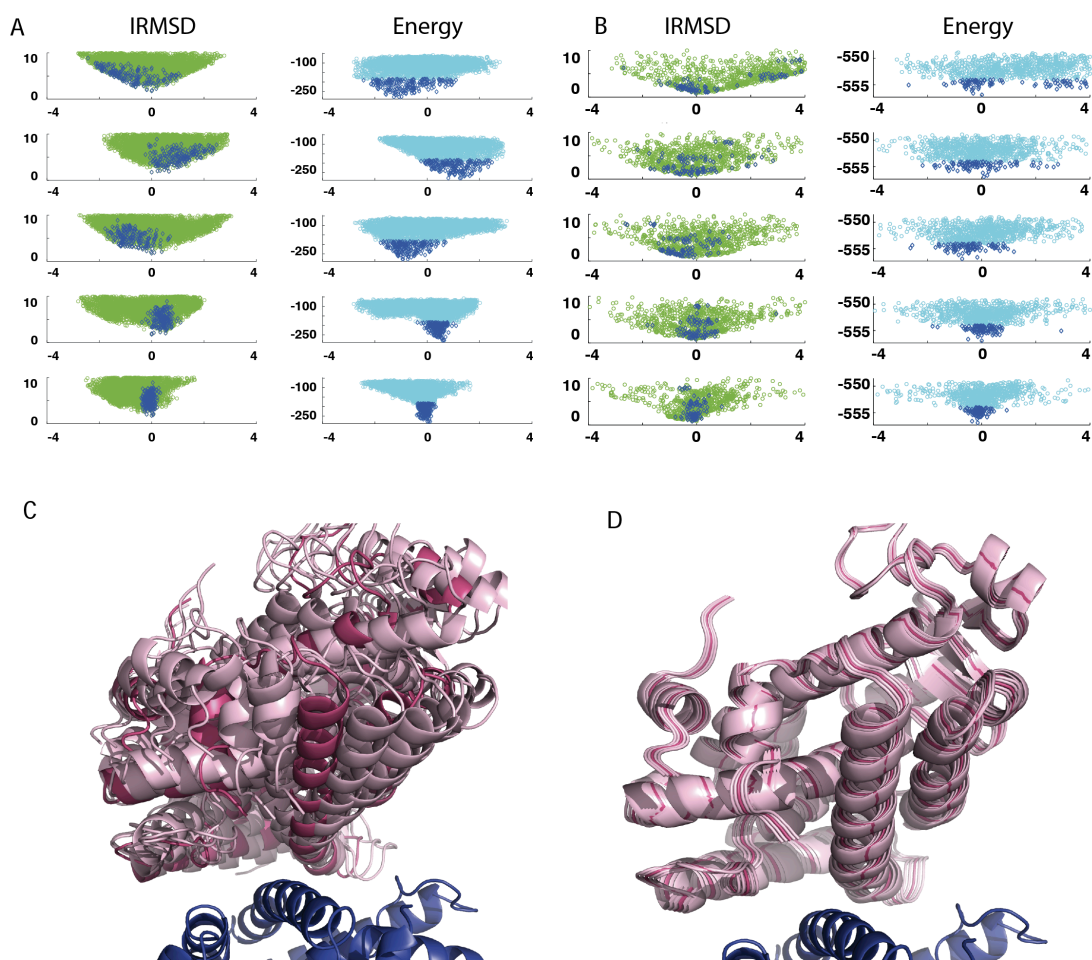


Figure 3 Shape of the energy landscape along the five PCA eigenvectors for the complex of PPAR- γ and RXR- α (PDB code 1K74). **(A)** Distributions of IRMSD (green) and energy (cyan) values based on structures generated by PIPER as functions of the “balanced” coordinates shown on the x-axis. Dark blue diamonds indicate low energy data points used for the PCA. The IRMSD (y-axis in the left column) is given in Å. The energy values (on the y-axis in the right column) are given by the PIPER scoring function. **(B)** Same as **Figure 3A**, but based on structures generated by RosettaDock. The energy values (on the y-axis in the right column) are given by the RosettaDock scoring function. **(C)** Encounter complexes along the most permissive direction v_1 . The ensemble includes mostly translations from the native state. **(D)** Encounter complexes along the most restrictive direction v_5 .

The following figure supplement is available for Figure 3:

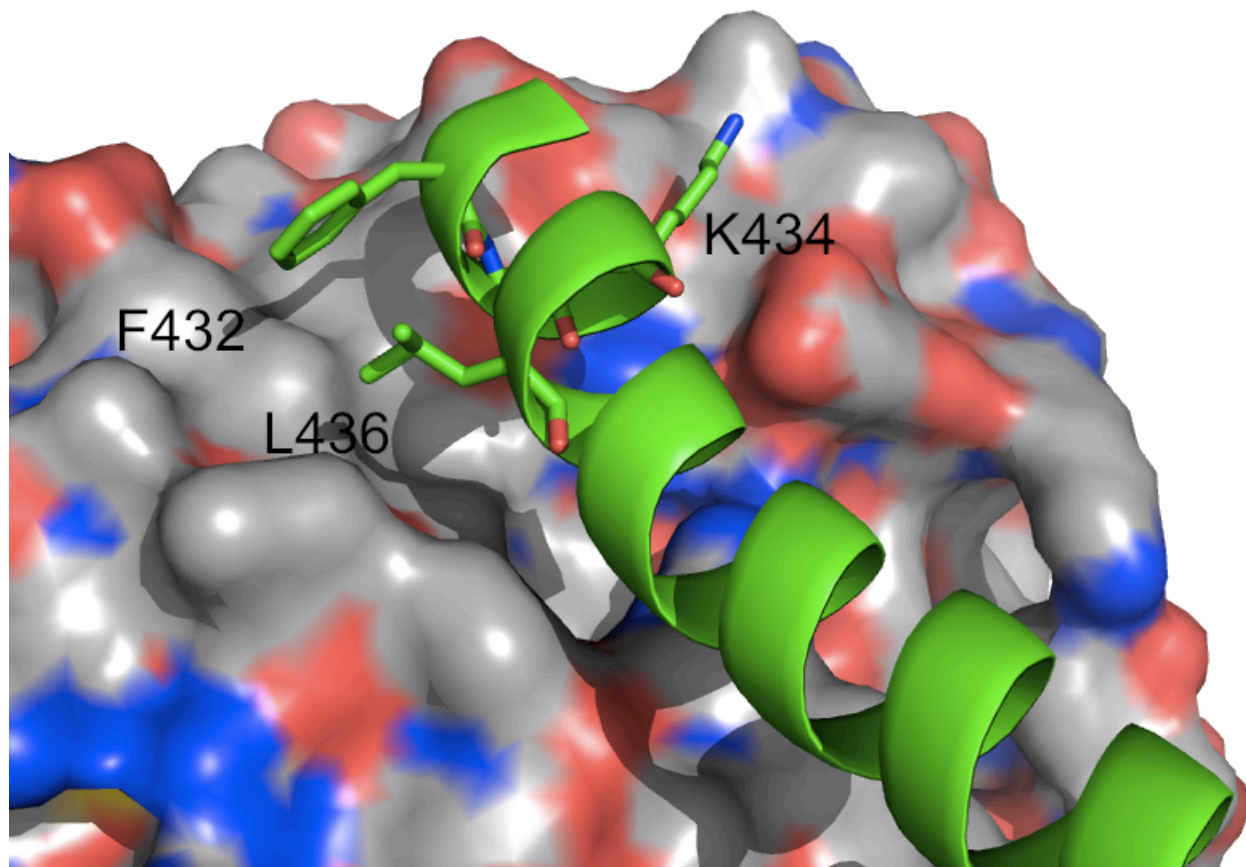


Figure supplement 1. Helix H12 of PPAR γ with residues of the hydrophobic patch indicated.

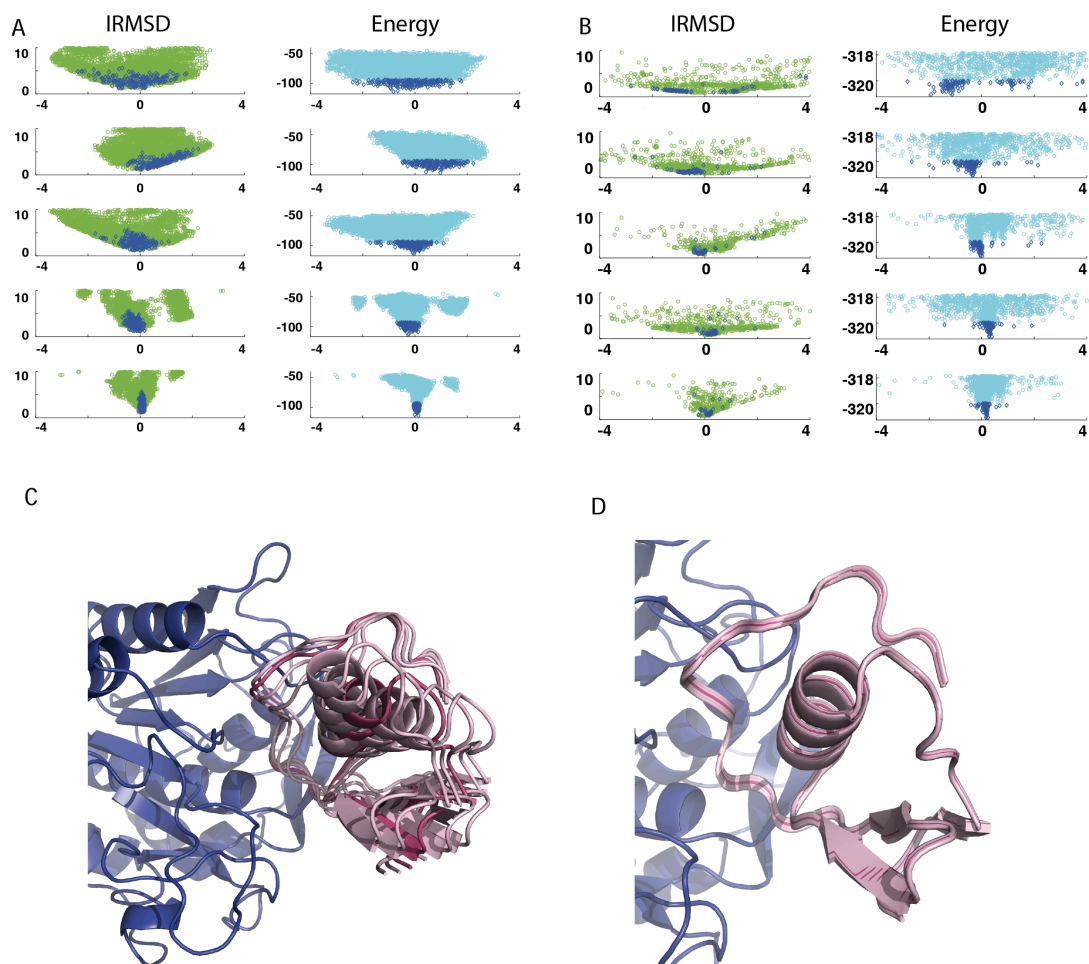


Figure 4. Shape of the energy landscape along the five PCA eigenvectors for the complex of subtilisin Carlsberg and its protein inhibitor, OMTKY3. All notations are as in **Figure 3**. **(A)** Distributions of interface IRMSD and energy values based on the structures generated by PIPER. **(B)** Same as **Figure 4A**, but based on the RosettaDock dataset. **(C)** Encounter complexes along the most permissive direction \mathbf{v}_1 . The ensemble consists of small rotations that leave the inhibitory loop position largely invariant. **(D)** Encounter complexes along the most restrictive direction \mathbf{v}_5 .

The following figure supplement is available for Figure 4:

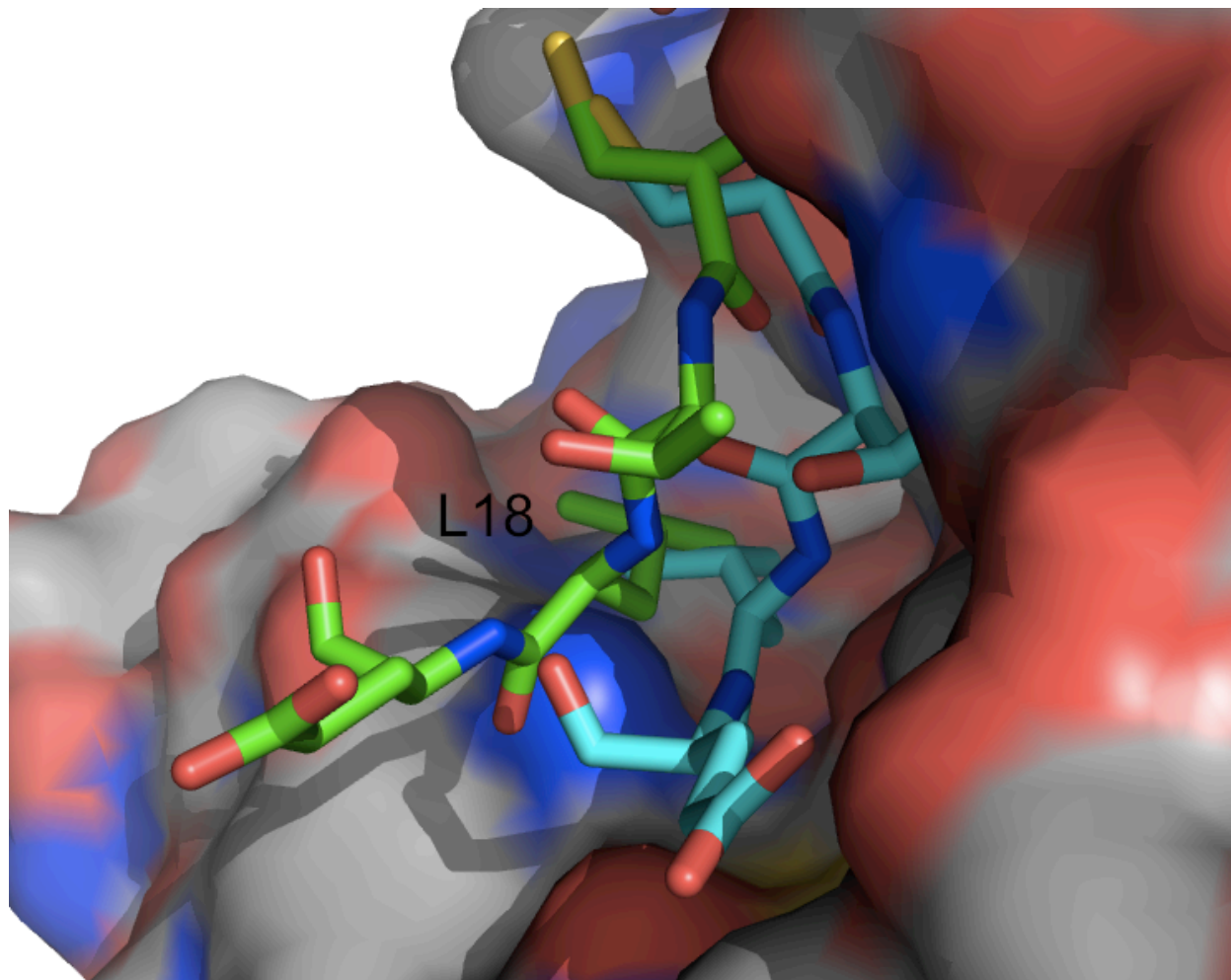


Figure supplement 1 Movement of the OMTKY3 inhibitory loop into the active site of subtilisin Carlsberg.

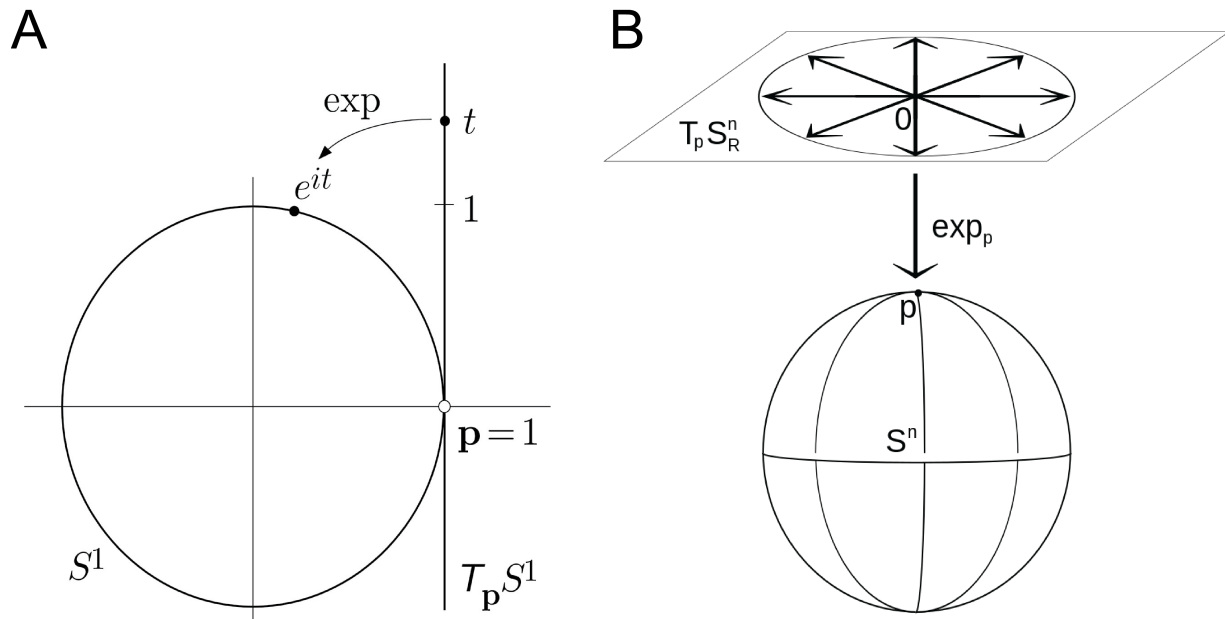


Figure 5 Examples of simple exponential maps. **(A)** Parameterization of the unit circle using an exponential map. The function e^{it} is a one-to-one mapping of the tangent line around $p=1$ onto the unit circle. Notice that singularity occurs only at $t=\pm\infty$. **(B)** Parameterization of the 3D unit sphere using exponential parameters.

Table 1. Eigenvalues (in %) obtained by PCA, and the angle between restrictive subspaces

PDB ID	PIPER					RosettaDock					Discrepancy (degrees)
	λ_1	λ_2	λ_3	λ_4	λ_5	λ_1	λ_2	λ_3	λ_4	λ_5	
1AVX	59.4	32.8	6.2	1.2	0.3	67.4	15.5	13.4	3.4	0.3	5
1B6C	72.1	19.1	6.9	1.3	0.5	84.2	10.2	3.3	1.9	0.4	4
1E6E	59.1	18.1	11.3	10.0	1.5	57.6	16.3	10.9	8.8	6.4	29
1EAW	44.3	31.7	22.2	1.0	0.9	57.9	33.0	4.6	4.0	0.4	25
1E6J	78.7	13.5	7.1	0.3	0.3	47.6	31.5	18.7	1.2	1.0	16
1GLA	58.9	26.9	9.3	3.7	1.2	41.5	33.1	15.1	8.0	2.3	2
1IQD	74.7	13.5	7.8	3.6	0.4	58.0	26.7	12.7	1.9	0.7	13
1K74	47.8	28.0	19.0	3.6	1.5	61.0	22.0	10.5	5.2	1.2	19
1MAH	60.3	22.4	11.7	4.4	1.2	52.8	22.0	13.5	7.7	4.0	14
1N8O	56.1	23.4	13.3	6.4	0.9	66.9	22.3	10.3	0.3	0.2	20
1PPE	56.4	26.4	14.9	1.7	0.6	47.1	44.4	7.9	0.4	0.1	3
1PXV	68.3	17.0	9.6	4.3	0.8	32.1	27.2	23.6	14.5	2.7	8
1R0R	55.0	26.8	15.3	2.7	0.2	69.3	20.2	6.7	3.0	0.9	13
2SNI	49.3	31.6	17.0	1.5	0.6	79.6	15.5	3.5	1.2	0.2	16
1KXQ	47.7	30.0	16.8	4.1	1.3	66.3	30.0	4.4	0.2	0.1	29
7CEI	44.7	28.5	20.9	4.6	1.3	47.7	27.9	18.9	3.6	1.9	19
2SIC	58.6	23.4	9.4	7.2	1.4	84.2	8.8	4.1	2.4	0.5	3
1AY7	56.9	20.3	15.0	5.4	2.4	42.1	32.5	12.6	9.2	3.7	27
1OPH	72.6	15.5	9.2	2.2	0.5	84.2	9.3	5.9	0.4	0.2	21
1UDI	64.6	18.6	12.6	2.4	1.8	51.2	27.1	14.2	6.4	1.1	33
1BUH	44.8	27.7	17.6	9.2	0.6	40.3	32.9	16.6	8.2	1.9	21
1FSK	45.0	28.0	22.1	3.5	1.4	42.6	29.7	19.9	5.8	1.9	21
1JPS	57.1	25.7	12.4	4.0	0.8	56.3	28.8	13.7	0.7	0.6	30
1DQJ	51.4	31.3	15.0	1.4	0.9	46.5	19.8	17.4	12.3	4.0	17
2B42	55.6	27.7	12.8	3.4	0.5	45.4	23.1	15.7	11.5	4.4	24
2FD6	65.1	18.1	9.9	4.6	2.2	36.4	23.9	21.0	13.7	5.0	20
2HQS	80.1	11.3	7.2	1.0	0.4	54.1	36.2	7.8	1.6	0.4	9
2I25	70.3	18.5	9.9	0.8	0.5	56.0	15.3	12.8	10.5	5.3	12
2MTA	45.8	26.1	20.5	5.2	2.5	45.5	32.2	12.2	7.4	2.7	30
1MLC	59.3	31.5	6.8	1.2	1.1	42.7	30.1	17.3	7.0	2.8	17
2HRK	57.7	31.0	9.7	0.9	0.7	61.2	16.4	10.5	8.6	3.3	30
1AHW	74.4	16.3	7.7	1.1	0.5	46.7	31.5	17.2	3.1	1.5	24
1Z5Y	66.1	18.0	8.9	5.4	1.5	57.1	32.3	9.7	0.6	0.4	29
2HLE	54.0	28.1	13.0	3.4	1.4	67.0	12.9	12.1	5.9	2.1	2
2NZ8	69.4	14.1	8.4	5.2	2.9	44.8	28.3	15.1	7.3	4.5	34
1BVN	61.4	20.3	14.3	3.6	0.4	37.2	28.5	17.8	10.0	6.5	32
1CGI	66.9	15.4	10.9	5.4	1.9	57.9	27.9	10.7	3.0	0.5	48
1GPW	53.8	20.9	14.2	6.4	4.7	46.5	26.5	17.9	5.0	4.0	27
2JEL	72.4	16.3	8.1	2.2	0.9	47.8	31.6	12.9	6.8	0.8	31
1NCA	76.7	18.8	3.0	1.2	0.4	55.9	24.3	15.6	3.2	1.0	27
2UUY	69.4	15.4	12.7	1.6	0.9	73.6	16.2	9.0	1.0	0.2	11
1KAC	48.9	34.6	13.3	2.0	1.2	53.8	19.5	15.6	6.8	4.2	30

Figure supplements:

Figure 1 Figure supplement 1 Rotamers of the paramagnetic labels E5C-EDTA-Mn²⁺ and E32C-EDTA-Mn²⁺ on HPr. The C-EDTA moiety is shown as sticks, with carbon atoms colored cyan. The rest of the HPr structure is shown as yellow cartoon. The Mn²⁺ ions are shown as magenta spheres. **(A)** Three rotamers of HPr-E5C-EDTA-Mn²⁺. **(B)** Three rotamers of HPr-E32C-EDTA-Mn²⁺.

Figure 2 Figure supplement 1 Controls emphasizing the need for accurate energy function in docking: theoretical PRE profiles for the EIN/HPr complex, based on complexes generated by using only the van der Waals energy (blue line). Theoretical intermolecular PREs, calculated from the coordinates of the specific EIN/HPr complex, are also shown as reference (black line). The experimental PRE rates (Γ_2) are displayed as filled-in magenta circles. **(A)** Results for EIN/HPr-E5C-EDTA-Mn²⁺ complexes. **(B)** Results for EIN/HPr-E32C-EDTA-Mn²⁺ complexes.

Figure 2 Figure supplement 2 Normalized intermolecular PRE profiles and encounter complexes for the IIA^{Mannitol} / HPr interactions. **(A)** Native structure of the complex formed by IIA^{Mannitol} (grey) and HPr (yellow). The location of the paramagnetic tag, HPr-E5C-EDTA-Mn²⁺, is colored red and is indicated by a circle. The PDB ID of the complex is 1J6T. **(B)** Centers of HPr structures, shown as blue spheres, in the encounter complex ensemble generated by the PIPER docking program. IIA^{Mannitol}, shown as grey solid, is considered the receptor. The native binding pose of HPr is shown as yellow cartoon. **(C)** Theoretical intermolecular PRE profiles calculated from the coordinates of the native structure only (black line), and based on all encounter complexes generated by the docking (blue line). The experimental PRE rates (Γ_2) are displayed as filled-in magenta circles (Tang et al. 2006). Points representing Γ_2 values that were too large (>60 s⁻¹) to be determined accurately are placed at the saturation level $\Gamma_2/\Gamma_{2max}=1$. The interface residues of IIA^{Mannitol} are indicated by red ticks on the x-axis.

Figure 2 Figure supplement 3. Normalized intermolecular PRE profiles and encounter complexes for the HPr / HPr interactions. **(A)** Normalized intermolecular PRE profiles for the HPr/HPr complex. The theoretical intermolecular PREs profile, calculated from low energy encounter complexes, is shown as a green line. The experimental PRE rates (Γ_2) are displayed as filled-in magenta circles (Tang et al. 2008). Points representing Γ_2 values that were too large (>60 s⁻¹) to be determined accurately are placed at the saturation level $\Gamma_2/\Gamma_{2max}=1$. Interface residues are indicated by red ticks on the x-axis. **(B)** Ensemble of low energy conformations of HPr / HPr interactions (Tang et al. 2008). One of the two HPr molecules, considered the receptor, is shown as grey cartoon. The centers of the other HPr positions generated by the

docking are shown as small blue spheres. These structures were used for back-calculating the theoretical PRE profile (green curve) shown in A.

Figure 2 Figure supplement 4 Encounter complexes in the Cytochrome c - Cytochrome c peroxidase interactions as reported on the basis of PRE experiments (**Bashir et al. 2010**), shown as pink spheres, and the ones generated by the PIPER docking program, shown as blue spheres.

Figure 3 Figure supplement 1 Helix H12 of PPAR γ with residues of the hydrophobic patch indicated. The receptor, RXR α , is shown in surface representation. Color code: oxygen red, nitrogen blue, and carbon white.

Figure 4 Figure supplement 1 Movement of the OMTKY3 inhibitory loop into the active site of subtilisin Carlsberg. Two snapshot of the motion are shown (in green and cyan) for residues 16 to 19 (CTLE), with L18 indicating the primary specificity residue.

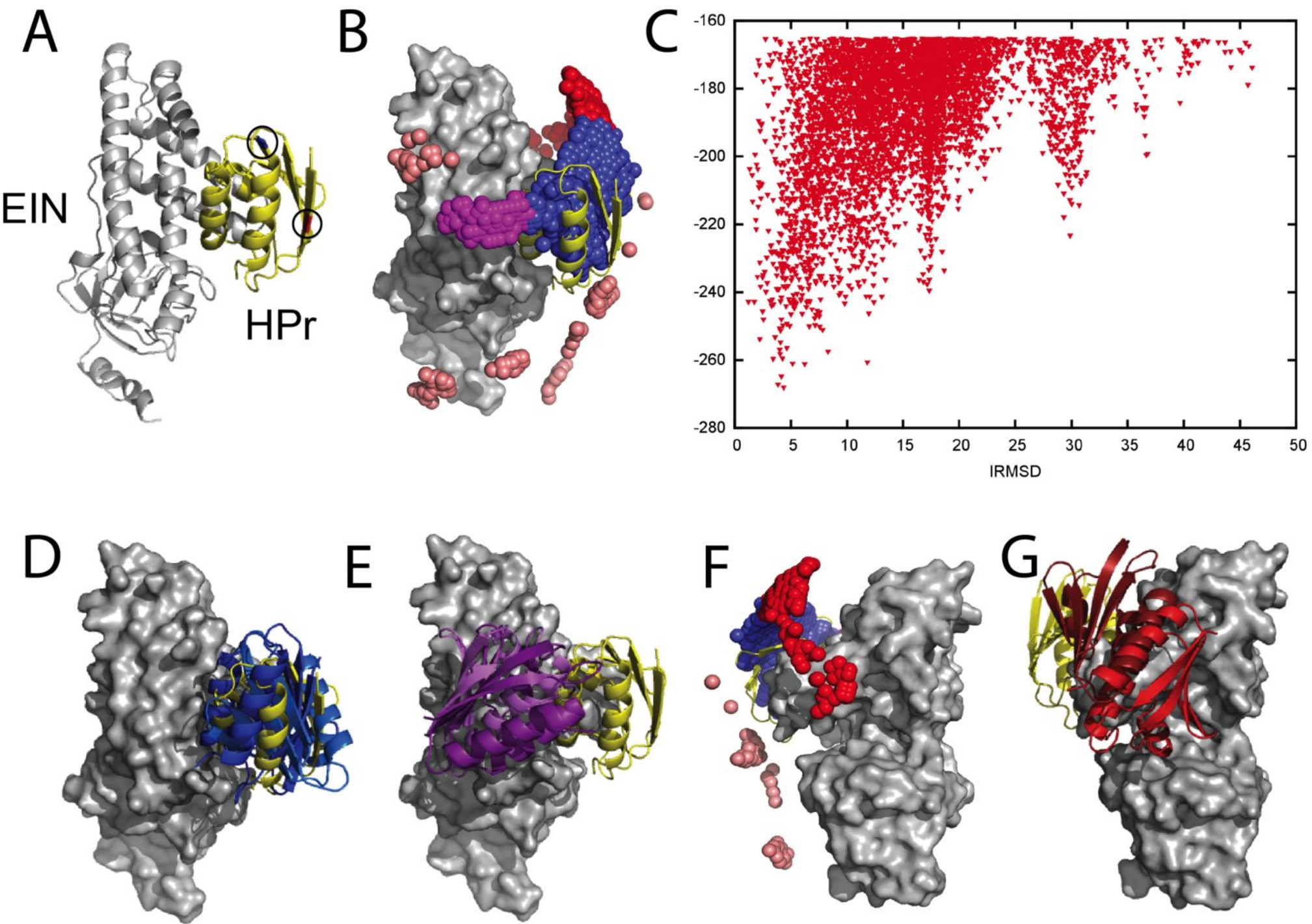
Rich media files

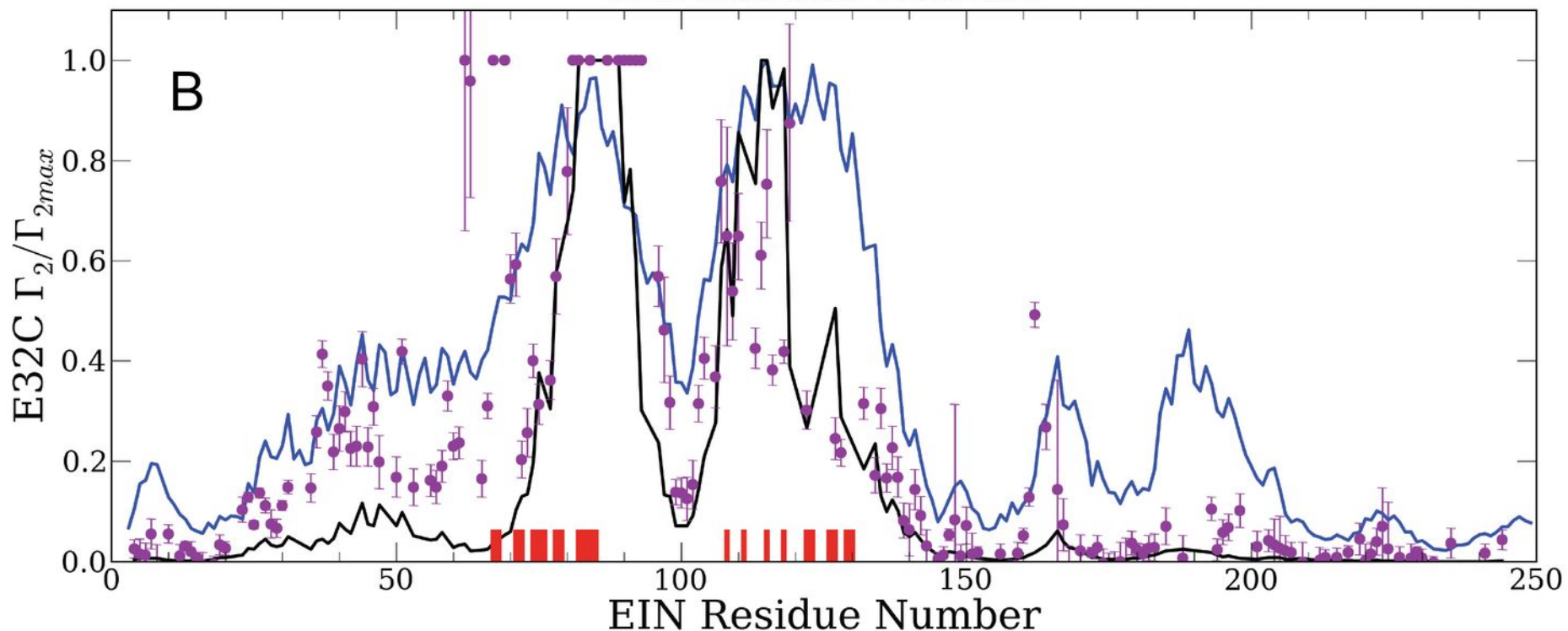
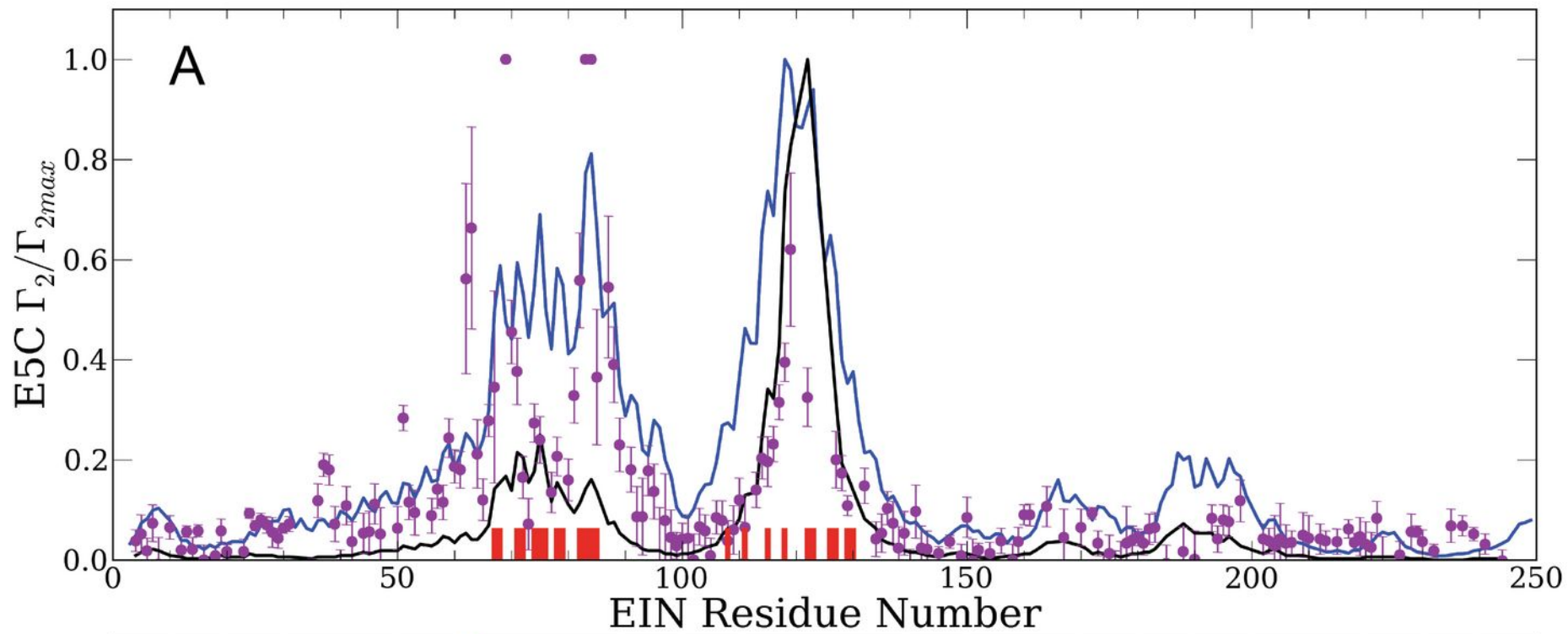
Video 1 Movement of PPAR γ , shown as green cartoon, along the most permissive eigenvector \mathbf{v}_1 . The receptor, RXR α , is shown as grey surface.

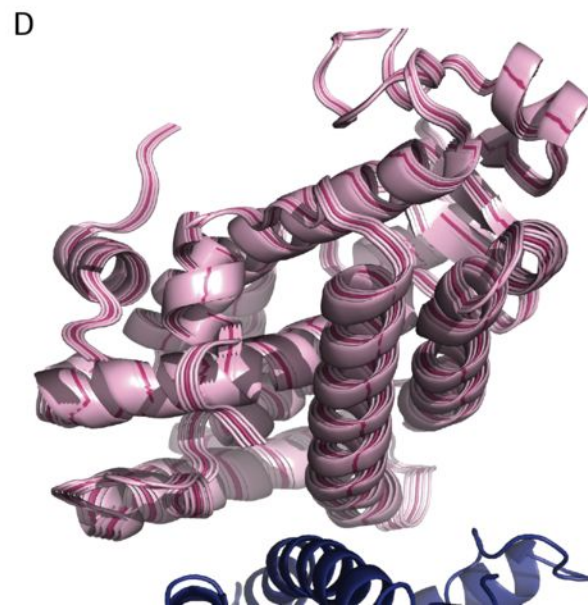
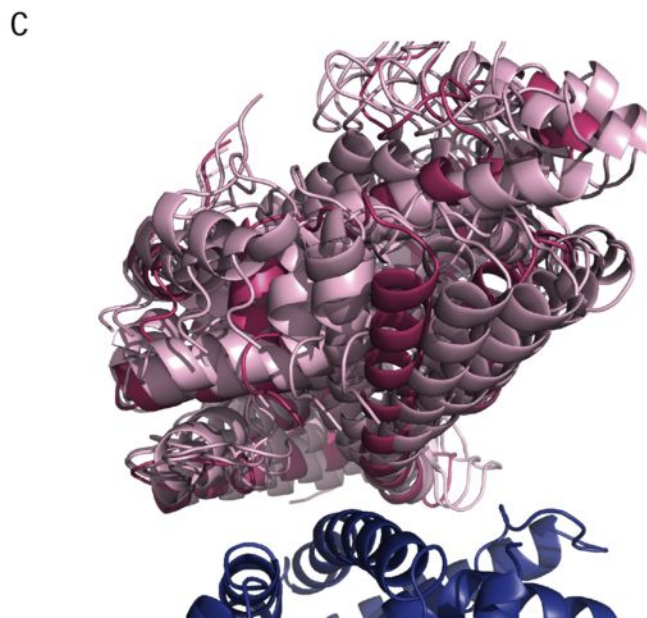
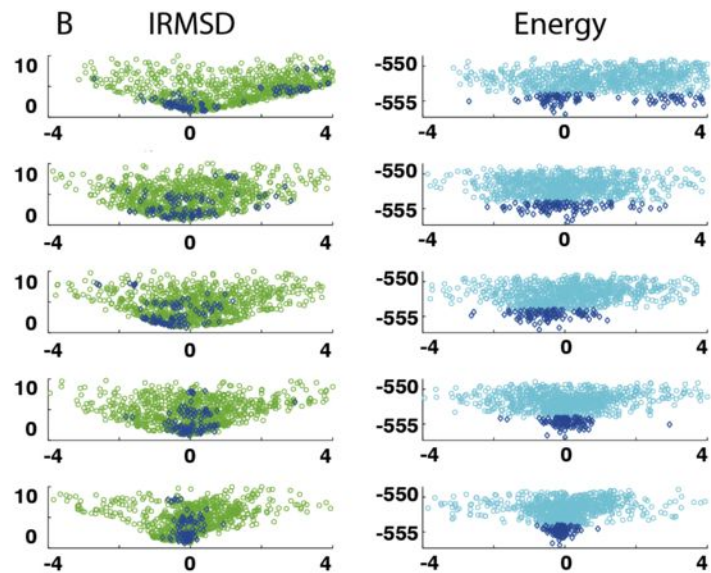
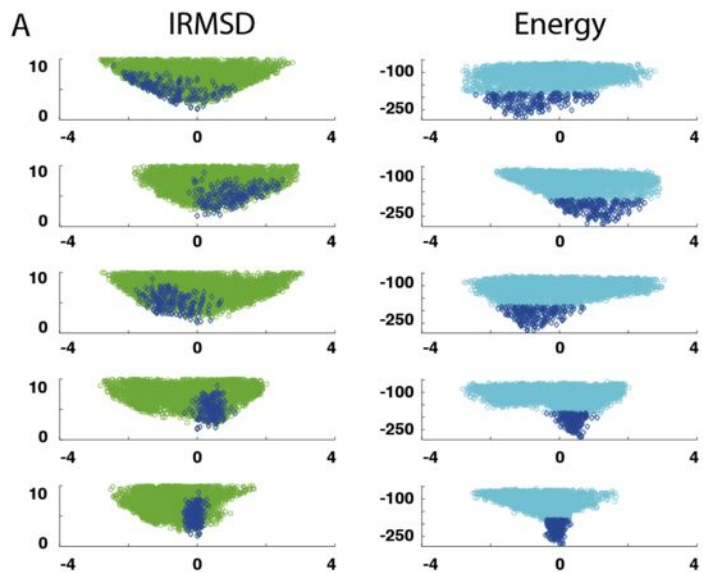
Video 2 Movement of PPAR γ , shown as green cartoon, along the second most permissive eigenvector \mathbf{v}_2 . The receptor, RXR α , is shown as grey surface.

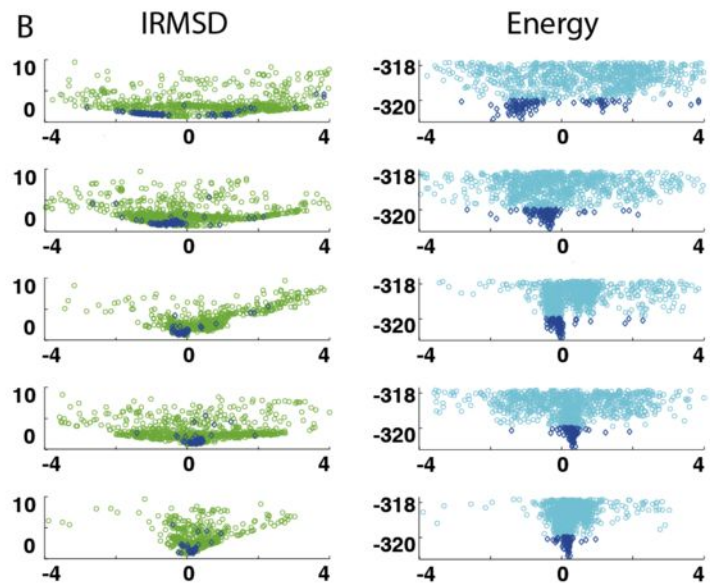
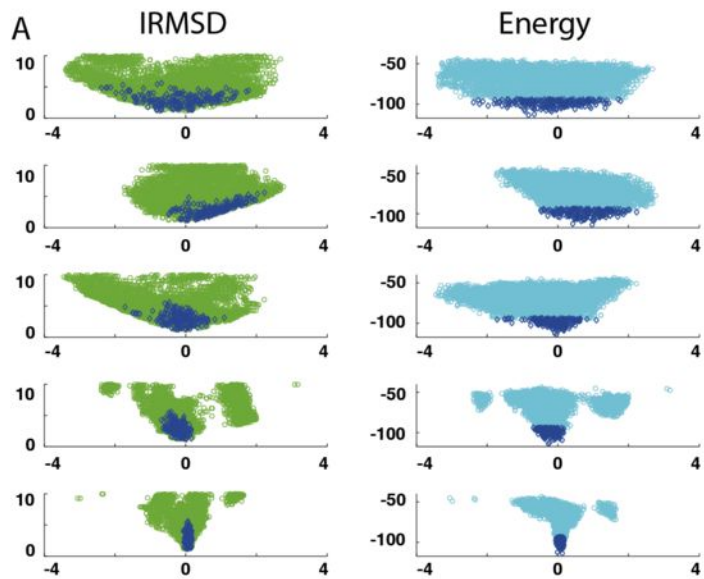
Video 3 Movement of the protein inhibitor, OMTKY3, shown as green cartoon, along the most permissive eigenvector \mathbf{v}_1 . The receptor, subtilisin Carlsberg, is shown as grey surface.

Video 4 Movement of the protein inhibitor, OMTKY3, shown as green cartoon, along the second most permissive eigenvector \mathbf{v}_2 . The receptor, subtilisin Carlsberg, is shown as grey surface.

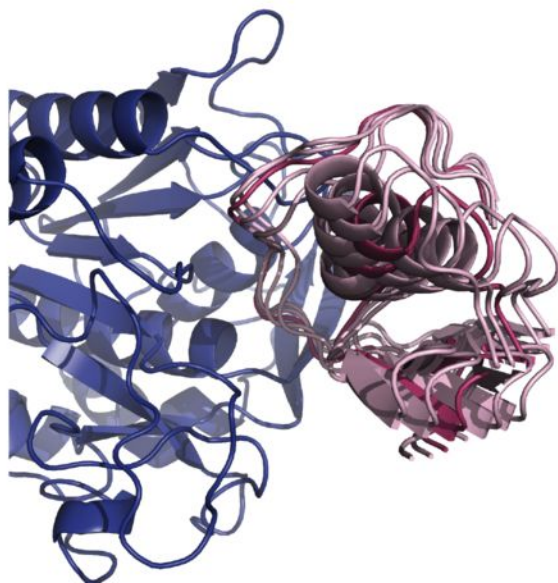




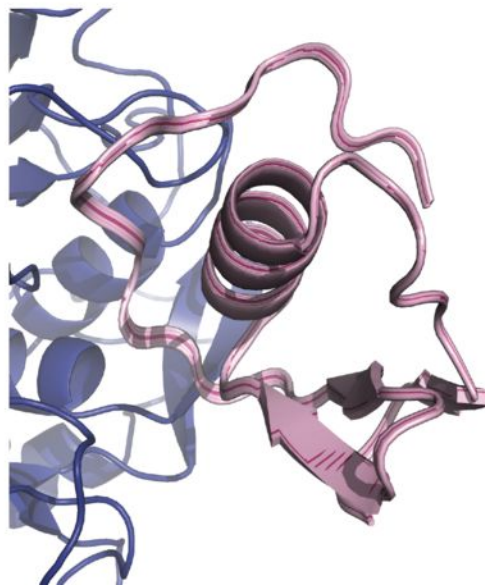




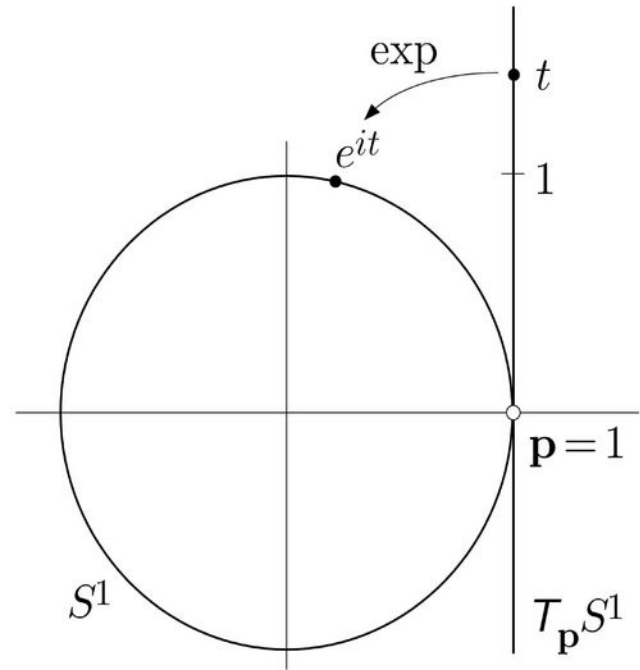
C



D



A



B

